PERGAMON

International Journal of Heat and Mass Transfer 46 (2003) 1063–1073

International Journal of HEAT and MASS TRANSFER

www.elsevier.com/locate/ijhmt

Lagrangian stochastic simulation of turbulent dispersion of heat markers in a channel flow

Y. Mito, T.J. Hanratty *

Department of Chemical Engineering, 205 Roger Adams Laboratory, University of Illinois at Urbana-Champaign, Box C-3, 600 South Mathews Avenue, Urbana, IL 61801, USA

Received 7 November 2001; received in revised form 28 August 2002

Abstract

A modified Langevin equation is developed to represent the dispersion of heat markers from point sources that originate at different locations in a channel through which a fluid is flowing turbulently. Of particular interest is the description of wall sources. Since a heated (or cooled) wall may be represented as a distribution of point sources (or sinks), these results can be used to describe heat transfer problems which have different configurations of heat transfer surfaces.

1. Introduction

A bulwark of turbulence theory has been Taylor's [1] description of the statistical behavior of a large number of fluid particles originating from a point source in a homogeneous isotropic turbulent field. However, its usefulness is limited because most turbulent fields are nonhomogeneous. Langevin [2] developed a treatment of Brownian motion, in which the force exerted by the molecules of the surrounding fluid consists of a damping term which varies linearly with the velocity of the particle and a rapidly varying stochastic term. Lin and Reid [3] and Obukhov [4] have shown that the Langevin equation gives the same result as Taylor's analysis if the Lagrangian correlation is represented by $\exp(-t/\tau)$, where τ is the Lagrangian time-scale.

A number of researchers have explored modifications of the Langevin equation which would allow for its use in nonhomogeneous fields [5–15]. Iliopoulos and Hanratty [16] tested the approach of Thomson [11] by comparing calculations for a source of fluid particles with experiments done in a direct numerical simulation (DNS) of turbulent flow in a channel. In these calculations, a non-Gaussian forcing function was used and a source of fluid particles was located at $x_2^+ = 40$, where x_2 is the distance from the wall and the plus superscript indicates that x_2 is made dimensionless using the friction velocity, v^*, and the kinematic viscosity, v. Mito and Hanratty [17] used a joint Gaussian distribution for the forcing function and studies of sources at different locations in a channel flow to give a more accurate specification of the spatial variation of the time-scale in the Langevin equation than was used by Iliopoulos and Hanratty [16].

This paper explores the possibility of using a modified Langevin equation to describe the dispersion of thermal markers. Of particular interest are the results for a point source (or a sink) located on the wall. This introduces a number of issues not considered in the analysis of the dispersion of fluid particles. The direct influence of molecular thermal diffusion needs to be considered not only because it adds to the dispersion but also because it is the mechanism by which the dispersing markers are removed from the wall. This is done by considering that the markers are displaced both by convection and by a random walk associated with molecular diffusion [18,19]. Because of molecular diffusion the marker need not follow a fluid particle. This effect is taken into account by allowing the time-scales in the Langevin equation to depend on the Prandtl number (or the Peclet number). Finally, it should be pointed out that a consideration of the behavior of wall sources provides a strong test of the ability of a modified

* Corresponding author. Tel.: +1-217-333-1318; fax: +1-217-333-5052.

E-mail address: hanratty@scs.uiuc.edu (T.J. Hanratty).

0017-9310/03/$ - see front matter
PII: S0017-9310(02)00362-9

Nomenclature

A	heat transfer area
c_p	specific heat at constant pressure
$d\mu_1$, $d\mu_2$	random forcing functions in the x_1, x_2 directions
$d\mu_1'$, $d\mu_2'$	fluctuating components of $d\mu_1$ and $d\mu_2$
k	thermal conductivity
K_b	heat transfer coefficient defined by using T_b, $= q_w/(T_b - T_w)$
K_c	heat transfer coefficient defined by using T_c, $= q_w/(T_c - T_w)$
h	half channel height
P	probability density function of heat markers
Pe_τ	Peclet number $= PrRe_\tau$
Pr	Prandtl number $= \rho c_p \nu/k$
Q	quantity of heat
q_w	heat flux at the wall
R_1, R_2	Lagrangian velocity autocorrelations
Re_τ	Reynolds number $= v^* h/\nu$
t	time
t^0	time instant at which heat markers are released
T	temperature
T^*	friction temperature $= q_w/\rho c_p v^*$
T_b	bulk fluid temperature
T_c	centerline temperature
T_w	wall temperature
$\tilde{u}_1$, $\tilde{u}_2$	velocity components in the x_1, x_2 directions
U_1	mean velocity component in the x_1 direction
u_1, u_2	fluctuating velocity components in the x_1, x_2 directions
v^*	friction velocity
w_1, w_2	Gaussian random numbers in the x_1, x_2 directions
x_1, x_2, x_3	streamwise, wall-normal, spanwise coordinates

Greek symbols

α_t	turbulent diffusivity $= -\overline{v\theta}/(dT/dy)$
ν	kinematic viscosity
θ	fluctuating temperature
ρ	density
σ_1, σ_2	turbulence intensities in the x_1, x_2 directions
σ_m	root-mean square of random walk
τ	Lagrangian time-scale in homogeneous isotropic turbulence
τ_1, τ_2	Lagrangian time-scales in the x_1, x_2 directions

Superscripts and subscripts

$\overline{(\ )}$	Eulerian average calculated from a DNS
$\langle\ \rangle$	ensemble average
$(\ )^+$	value made dimensionless with wall parameters
$(\ )^n$, $(\ )^{n+1}$	values at the nth and $(n+1)$th time steps

Langevin equation to describe dispersion in an inhomogeneous field.

The system considered is fully developed turbulent flow in a channel at $Re_\tau = 150$, where the Reynolds number is defined using the friction velocity and the half-height of the channel. The calculated results are evaluated by comparing them with experiments carried out in a DNS. Studies were made for $Pr = 0.1$, 0.3 and 1 for point sources located at $x_2^+ = 0, 1, 2, 5, 10, 20, 40, 70, 100, 130, 150$.

A principal motivation for this study is the description of turbulent heat transfer from a wall by Lagrangian methods. Papers by Hanratty [20] and by Papavassiliou and Hanratty [21,22] have shown how temperature fields can be calculated by considering a hot wall as an array of point sources of heat. This provides a more fundamental way to understand the physics of turbulent transfer than does an Eulerian method. For example, the measured spatial variation of Eulerian turbulent diffusivities can be interpreted as being related to the time dependency of the dispersion of heat from a wall source. Furthermore, the Lagrangian approach can sometimes provide a more robust way of doing heat transfer calculations. For example, Papavassiliou and Hanratty [21] have shown that a DNS of a turbulent flow can be used to calculate heat transfer at arbitrarily large Prandtl numbers by using Lagrangian methods.

Therefore, the calculations for dispersion from wall sources are used to calculate the fully developed temperature field that results when a fluid flows through a channel in which one wall is heated and one wall is cooled. The hot wall is considered to be an array of heat sources and the cold wall, as an array of heat sinks. The rate of heat transfer at both walls are the same so that, under fully developed conditions, the heat flux, q_w, does not vary with x_2. Heat transfer coefficients, K_b and K_c, are defined as

$$q_w = K_b(T_b - T_w) = K_c(T_c - T_w), \tag{1}$$

where T_b is the bulk fluid temperature and T_c is the centerline temperature.

2. Lagrangian experiments in the DNS

A pseudospectral fractional step method [23] was used to calculate the turbulent velocity field. The di-

mensions of the channel were 1900 v^*/v, in the streamwise direction (x_1) and 950 v^*/v in the spanwise direction (x_3). The computational grid was $128 \times 65 \times 128$. The resolutions were $\Delta x_1^+ = 15$, $\Delta x_3^+ = 7.4$ and $\Delta x_2^+ = 0.18$ at the wall to 7.4 at the center. No slip boundary conditions were used at $x_2^+ = 0$, 300, and periodicity was assumed in the x_1 and x_3 directions. The time step was $\Delta t^+ = 0.25$.

The tracking method used to follow fluid particles or thermal markers is described in papers by Kontomaris et al. [24] and by Kontomaris and Hanratty [19]. The displacements of heat markers are calculated as the sum of an advective component and a molecular diffusive component:

$$\mathrm{d}x_i = (U_i + u_i)\,\mathrm{d}t + \sigma_\mathrm{m} w_i, \tag{2}$$

where U_i and u_i are the mean and fluctuating velocity at the location of the heat source and w_i is a random displacement defined by a Gaussian probability distribution function. The dimensionless root-mean square of the displacements associated with molecular diffusion is given by $\sigma_\mathrm{m}^+ = \sqrt{2\mathrm{d}t^+/Pr}$ where $\mathrm{d}t^+$ is the dimensionless time interval. Because of the homogeneity in the x_1 and x_3-directions, studies of dispersion from a source at a given x_2 were carried out by using 16,129 sources that were uniformly distributed over the x_1–x_3 plane. The Lagrangian calculation was performed over a time period of 400 v/v^{*2}. The time step for the tracking was 0.25 v/v^{*2}.

The bounce condition (perfectly elastic collision) was used when a thermal marker hit the wall. This is equivalent to enforcing the boundary condition of an adiabatic wall [18]. Three runs were made by using different initial flow fields that were separated by time intervals of about 200 v/v^{*2}, so that a total of 48,387 trajectories were used. The DNS results for the behavior of a single wall source obtained by Papavassiliou and Hanratty [21,22] over a time period of 2750 v/v^{*2} were used to calculate the fully developed temperature field. The method for doing this is explained in Section 4.2.

3. Langevin equation

In a Lagrangian stochastic simulation a Langevin equation, rather than a DNS, is used to calculate fluid velocities at locations of heat markers. The displacements of heat markers are calculated with (2). A modified Langevin equation which specifies the change of u_i over the interval $\mathrm{d}t$ is given as

$$\mathrm{d}\left(\frac{u_i}{\sigma_i}\right) = -\frac{u_i}{\sigma_i \tau_i}\,\mathrm{d}t + \overline{\mathrm{d}\mu_i} + \mathrm{d}\mu_i', \tag{3}$$

where τ_i is the Lagrangian time-scale and $\mathrm{d}\mu_i$ is a random forcing function which consists of a mean drift $\overline{\mathrm{d}\mu_i}$ and a fluctuation $\mathrm{d}\mu_i'$. (Since a fully developed condition will be assumed, the time mean and the ensemble mean are equal.) The Eulerian root-mean square of the velocity fluctuation in the i-direction, σ_i, which is calculated from the DNS, is introduced in (3), as suggested by Thomson [11]. The Einstein convention of summing over repeated indices is not used. The specification of τ_i is discussed in Section 6.1. The mean drift $\overline{\mathrm{d}\mu_i}$ is obtained by taking an ensemble average of (3) for a large number of trajectories:

$$\overline{\mathrm{d}\mu_i} = \frac{\partial(\overline{u_2 u_i}/\sigma_i)}{\partial x_2}\,\mathrm{d}t, \tag{4}$$

where the overbar indicates an Eulerian average obtained from the DNS.

The covariances of the random forcing functions $\mathrm{d}\mu_i'$ are obtained by using the definition of a stochastic differential [16]:

$$\overline{\mathrm{d}\mu_i' \mathrm{d}\mu_j'} = \left\{ \frac{\partial(\overline{u_i u_j u_2}/\sigma_i\sigma_j)}{\partial x_2} + \frac{\overline{u_i u_j}}{\sigma_i \sigma_j}\left(\frac{1}{\tau_i} + \frac{1}{\tau_j}\right)\right\}\mathrm{d}t + o(\mathrm{d}t)^2. \tag{5}$$

The random forcing function $\mathrm{d}\mu_i'$ is assumed to be jointly Gaussian. The use of a non-zero value of the correlation $\overline{\mathrm{d}\mu_1' \mathrm{d}\mu_2'}$ has been shown by Mito and Hanratty [17] to improve the calculation of the streamwise dispersion of fluid particles but not to affect the calculation of dispersion in the wall-normal direction. The triple correlation in (5) is taken to be zero. This is needed for the modified Langevin equation to fulfill the condition of well-mixedness [17] when an assumption of a joint Gaussian function is used for the forcing function.

4. Numerical methods

4.1. Time advancement scheme for the Lagrangian stochastic simulation

Initial conditions x_i^0 and $\tilde{u}_i^0$ for the simulation are specified from an instantaneous field obtained from the DNS. Trajectories of heat markers are calculated by integrating (2) by using the first-order Euler explicit method at the first time step and the second-order Adams–Bashforth method after that step. The fluid velocities at the locations of heat sources $\tilde{u}_i$ are calculated by using the fully implicit method.

$$\tilde{u}_i^{n+1} = \tilde{u}_i^n + \mathrm{d}U_i^{n+1} + \mathrm{d}u_i^{n+1}, \tag{6}$$

where $\mathrm{d}u_i^{n+1}$ is calculated with the modified Langevin equation,

$$\mathrm{d}u_i^{n+1} = u_i^{n+1}\left(-\frac{\mathrm{d}t}{\tau_i^{n+1}} + \frac{\mathrm{d}\sigma_i^{n+1}}{\sigma_i^{n+1}}\right) + \sigma_i^{n+1}\left(\overline{\mathrm{d}\mu_i}^{n+1} + \mathrm{d}\mu_i'^{n+1}\right), \tag{7}$$

where $dU_i^{n+1} = U_i^{n+1} - U_i^n$ and $d\sigma_i^{n+1} = \sigma_i^{n+1} - \sigma_i^n$. The superscripts, n and $n+1$, represent the times, t^n and t^{n+1}, at which these variables are calculated. By substituting $u_i^{n+1} = u_i^n + du_i^{n+1}$ into (7), du_i^{n+1} is obtained as

$$du_i^{n+1} = \left\{ u_i^n \left(-\frac{dt}{\tau_i^{n+1}} + \frac{d\sigma_i^{n+1}}{\sigma_i^{n+1}} \right) + \sigma_i^{n+1} \left(\overline{d\mu_i}^{n+1} + d\mu_i'^{n+1} \right) \right\} \Big/ \left(1 + \frac{dt}{\tau_i^{n+1}} - \frac{d\sigma_i^{n+1}}{\sigma_i^{n+1}} \right). \quad (8)$$

This fully implicit treatment stabilizes the time advancement in the stochastic simulation of heat markers by avoiding extremely large (nonphysical) velocity fluctuations in the near-wall region. This problem does not arise in the simulation of fluid particles [11,17], so a partially explicit method could be used in solving the velocities of fluid particles.

4.2. Calculation of fully developed temperature profiles

The motivation for the present study is the use of Lagrangian methods to calculate mean temperature profiles. In this approach, a hot wall is represented by a number of sources of heat and a cold wall is represented by a number of sinks of heat. The method for doing this is outlined in a paper by Papavassiliou and Hanratty [21]. Different types of configurations can be considered. Finite or infinitely long heated (and /or cooled) walls can be used. The wall can have a constant heat flux or a constant temperature. Papavassiliou and Hanratty [21] successfully used data for a point source obtained from experiments in a DNS to describe fully developed temperature profiles with constant temperature walls. To complete the present paper, the results from the Langevin representation of point sources are used to calculate temperature fields for a constant heat flux wall.

Since only fully developed temperature fields will be calculated, an infinitely long heated (or cooled) wall will be considered. The goal is to use the probability density functions for instantaneous sources to calculate the temperature of the fluid. Because the heated wall is infinitely long, temperatures will vary only with time and with x_2^+. Heating is started at time zero with the introduction of an instantaneous source with a strength

$$dQ = Aq_w\,dt, \quad (9)$$

where A is the heat transfer area and q_w is rate of heat transfer per unit area. At some time later the heat is distributed uniformly over the channel cross-section. The amount of heat in a bin of thickness dx_2 is $\rho c_p\,dT A dx_2$. The probability of a heat particle being located at a given x_2 is

$$\text{Probability} = \frac{\rho c_p\,dT A dx_2}{Aq_w dt}. \quad (10)$$

The probability distribution function $P(x_2,t)$ is thus related to the temperature distribution as follows:

$$P(x_2,t) = \frac{\rho c_p dT}{q_w dt}. \quad (11)$$

This can be made dimensionless using v^*, ν and a friction temperature $T^* = q_w/\rho c_p v^*$. Thus

$$dT^+ = P^+ dt^+. \quad (12)$$

Eq. (12) gives the temperature at a given time t^+ that results from an instantaneous wall source that entered the field between t_1^+ and $t_1^+ + dt^+$, where $0 \leqslant t_1^+ < t^+$. The contribution to the temperature from all the instantaneous sources is, therefore, given as

$$T^+ = \int_0^{t^+} P^+(x_2^+, t_1^+)\,dt_1^+. \quad (13)$$

This equation relates $T^+(x_2^+, t^+)$ to the probability density functions for the case in which the heat flux q_w is constant. If a solution for a constant temperature wall is sought then $q_w(t_1^+)$ needs to be a function of time. It is convenient to define $q_w(t_1^+) = w(t_1^+)q_{wr}$ where q_{wr} is some reference heat flux. Eq. (13) is then changed to

$$T^+ = \int_0^{t^+} w(t_1^+)P^+(x_2^+, t_1^+)\,dt_1^+, \quad (14)$$

where the friction temperature is defined using the converged temperature profile and $w(t_1^+)$ is selected so that T_w^+ is constant.

Values of T^+ were calculated from (13) and the probability distribution functions. A singularity in P^+ exist at $t^+ = 0$, whereby $P^+ \to \infty$. Therefore, an analytical solution for P^+ that considers only molecular transport was used from $t^+ = 0$ to 0.25:

$$T^+ = \sqrt{4t^+ Pr}\ \text{ierfc}\frac{x_2^+}{\sqrt{4t^+/Pr}}. \quad (15)$$

Eq. (15), which considers only molecular conduction, is given in Carslaw and Jaeger [25].

5. Results of Lagrangian experiments in the DNS

5.1. Lagrangian correlation coefficients

Lagrangian correlations were determined from the DNS of dispersion from point sources by calculating the ensemble mean, over a large number of trajectories, of the product of the fluid velocity at the locations of a thermal marker at times t and t^0, where the marker is introduced into the field at t^0. These need not be the same as for fluid particles because the marker can escape from the fluid particle by molecular diffusion. To be

consistent with the Langevin analysis, a Lagrangian correlation coefficient is defined as

$$R_i(x_2^+, t^n) = \frac{\langle (u_i^0/\sigma_i^0)(u_i^n/\sigma_i^n)\rangle}{\langle (u_i^0/\sigma_i^0)^2\rangle^{1/2}\langle (u_i^n/\sigma_i^n)^2\rangle^{1/2}}. \quad (16)$$

Here, the velocities are normalized with the rms of the local velocity fluctuations determined in an Eulerian framework and the brackets represent an ensemble average.

Values of R_1 and R_2 are presented in Fig. 1 for $Pr = 1$. The time, t, has been made dimensionless with wall parameters. Results are presented for experiments in which the source is located at different dimensionless distances from the wall. The Lagrangian correlation for R_1 decays more slowly than the correlation for R_2. Both R_1 and R_2 decay more rapidly for sources located closer to the wall. The correlations show a parabolic shape for very small t^+, which scales with the Kolmogorov time-scale [26]. These results are close to what has been obtained for fluid particles [17].

Fig. 2 presents calculated values of R_1 and R_2 for $Pr = 0.1$. These are found to be smaller than observed for $Pr = 1$ and for fluid particles. Furthermore, the correlations show an exponential decay at small t^+. These results show that the ability of thermal markers to follow the fluid turbulence decreases with decreasing Pr.

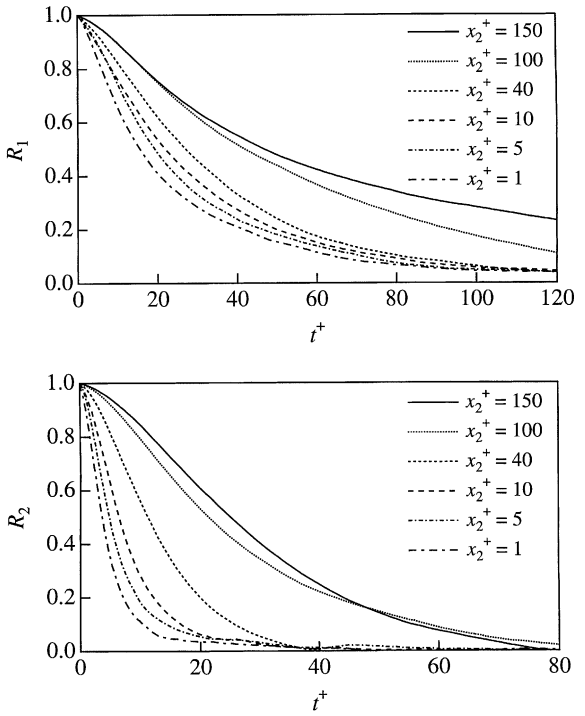

Fig. 1. Lagrangian velocity autocorrelation seen by heat sources with $Pr = 1$.

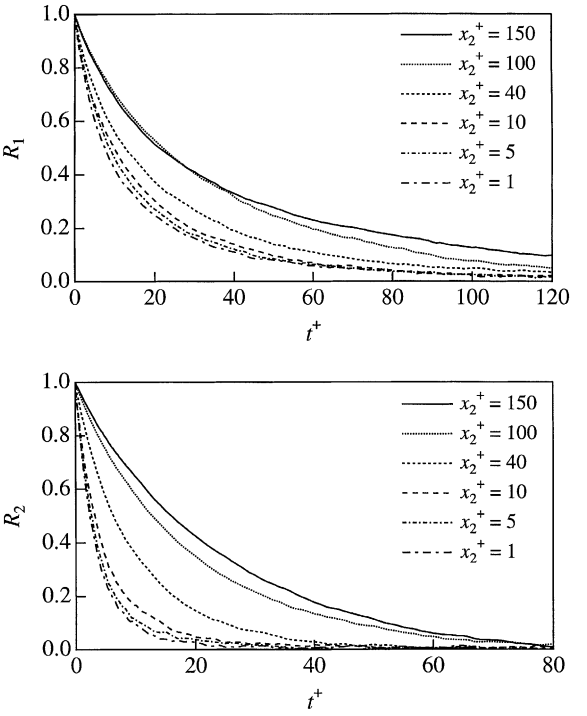

Fig. 2. Lagrangian velocity autocorrelation seen by heat sources with $Pr = 0.1$.

5.2. Dispersion of heat sources at $x_2^+ = 40$

The concentration profiles of hot particles characterized by $Pr = 1$ are shown in Fig. 3a for an instantaneous source that was introduced into the fluid at $t^+ = 0, x_2^+ = 40$. The solid curves are the results obtained from the DNS. These were calculated by using 40 equispaced bins in the region where the heat markers are located. The results are jagged, particularly at large times, because the number of samples was not large enough.

For small t^+ the concentration profile has a maximum close to $x_2^+ = 40$. However, at $t^+ = 25$ the profile is seen to be asymmetric. The hot particles disperse more rapidly in the positive direction because the wall-normal velocity fluctuations are greater for $x_2^+ > 40$ than for $x_2^+ < 40$. Because of the zero flux condition the heat particles pile up at the wall. A peak is located at the wall at $t^+ \cong 200$.

The effect of an increase in thermal conductivity on the wall-normal dispersion is displayed by comparing results for $Pr = 0.1$ in Fig. 3b with results for $Pr = 1$ in Fig. 3a. The decrease in Pr causes a much more rapid dispersion because the direct contributions of molecular diffusivity are larger. The maximum in the neighborhood of $x_2^+ = 40$ is smaller and it disappears at a smaller t^+.

Streamwise dispersions of hot particles admitted in the fluid at $x_2^+ = 40$, $t^+ = 0$, $x_1^+ = x_1^{0+}$ are presented in

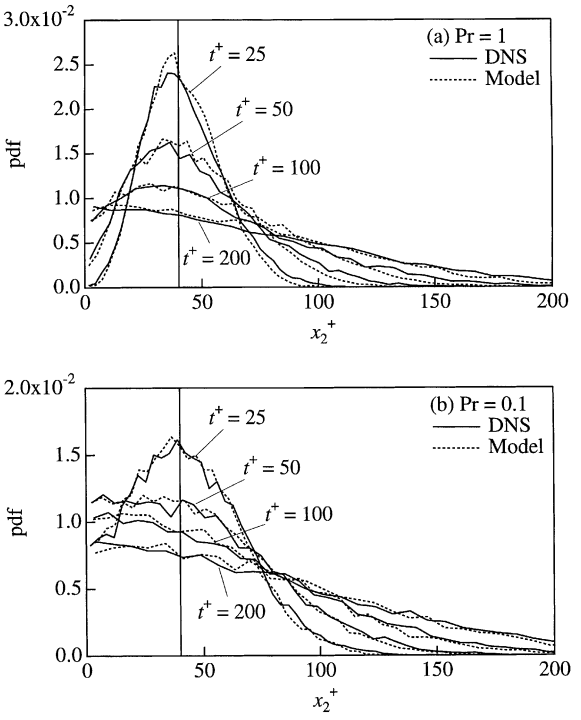

Fig. 3. Wall-normal dispersion of heat sources released at $x_2^+ = 40$ for (a) $Pr = 1$ and (b) $Pr = 0.1$.

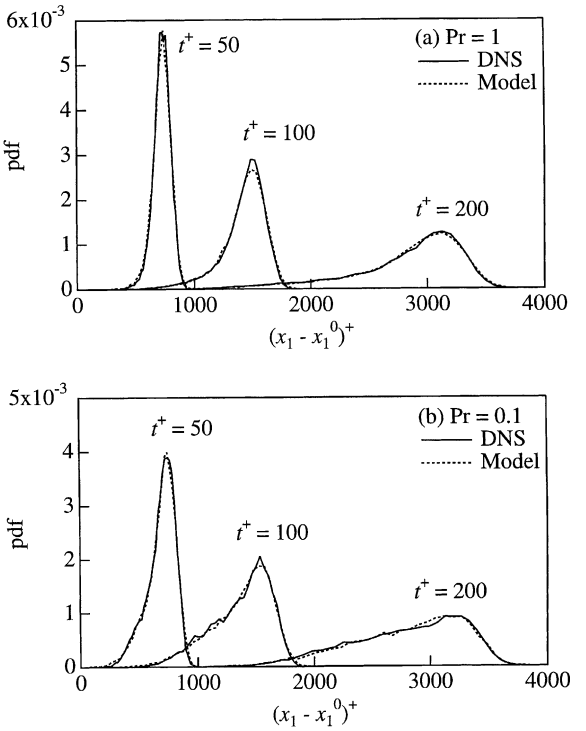

Fig. 4. Streamwise dispersion of heat sources released at $x_2^+ = 40$ for (a) $Pr = 1$ and (b) $Pr = 0.1$.

Fig. 4 for $Pr = 1$ and $Pr = 0.1$. Again, concentration profiles were calculated by using 40 equispaced bins. The concentrations at a given $(x_1 - x_1^0)^+$ include particles at all x_2^+. The hot particles are transported downstream by the mean velocity. The peaks are located at approximately the same $(x_1 - x_1^0)^+$ for $Pr = 1$ and for $Pr = 0.1$. However, the dispersions around the peaks are quite different. The larger dispersion for $Pr = 0.1$ is manifested by smaller peaks and a wider spread of the hot particles. Because more hot particles are accumulated in the slower moving fluid near the wall for $Pr = 0.1$ than for $Pr = 1$ (see Fig. 3) larger concentrations are observed for small $(x_1 - x_1^0)^+$. However, longer upstream tails are observed for $Pr = 1$ than for $Pr = 0.1$ at large t^+ because particles trapped very close to the wall have a greater difficulty to escape because of the smaller molecular diffusivity.

5.3. Dispersion from instantaneous wall sources

Of particular importance to the goal of the paper are the results for a wall source shown in Fig. 5. At small times hot particles disperse from the wall source by molecular diffusion. As they diffuse out to larger distances from the wall, turbulent velocity fluctuations play a more important role. Noting that the scale on the ordinate is smaller for $Pr = 0.1$ than for $Pr = 1$, we observe that the dispersion is much greater for $Pr = 0.1$. The dominance of molecular diffusion in dispersing hot

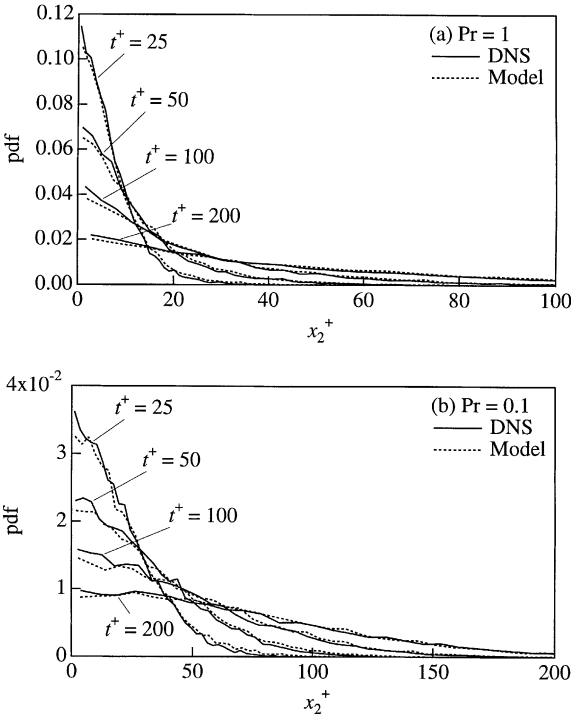

Fig. 5. Wall-normal dispersion of wall sources for (a) $Pr = 1$ and (b) $Pr = 0.1$.

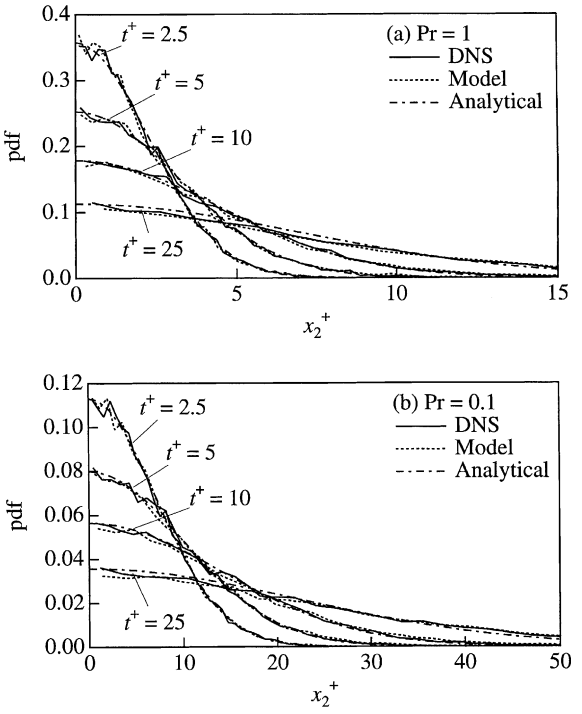

Fig. 6. Wall-normal dispersion of wall sources at small times for (a) $Pr = 1$ and (b) $Pr = 0.1$.

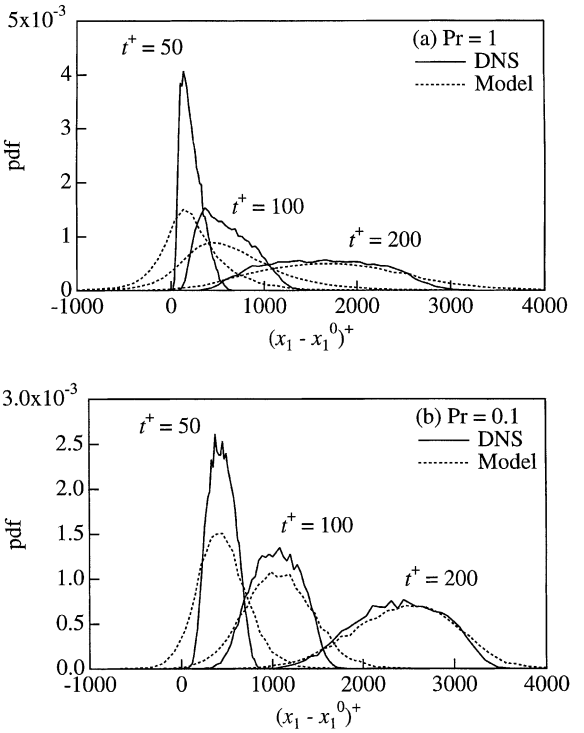

Fig. 7. Streamwise dispersion of wall sources for (a) $Pr = 1$ and (b) $Pr = 0.1$. Effect of streamwise velocity fluctuation was included.

particles away from the wall at small t^+ is illustrated in Fig. 6.

The curves with a dot and a dash represent the probability distribution functions calculated for a conducting medium given in Carslaw and Jaeger [25] as

$$P^+ = \frac{1}{\sqrt{\pi t^+/Pr}} \exp\left(-\frac{x_2^{+2}}{4t^+/Pr}\right), \tag{17}$$

where P^+ is doubled by taking account of the bounce condition of particles at the wall. The solid curves represent calculations done in the DNS of a turbulent field. The results are quite close to (17) for $t^+ \leqslant 10$ and start to deviate from (17) at $t^+ = 25$.

Streamwise dispersions of hot particles originating from a wall source are shown in Fig. 7. The solid curves represent calculations done in the DNS. Since the particles diffuse away from the wall faster for $Pr = 0.1$, they experience higher fluid velocities sooner. Consequently, the peaks are located farther downstream for $t^+ = 50$ and for $t^+ = 100$.

6. Results from the stochastic model

6.1. Definition of the Lagrangian time-scale

The use of the modified Langevin equation to model possible paths of particles from heat sources requires the Eulerian statistics, which are obtained from the DNS, and the definition of a Lagrangian time-scale which is obtained from the correlation coefficients shown in Figs. 1 and 2. We follow the approach taken by Mito and Hanratty [17] to define τ_i as the value of t at which $R_i = 0.368$. These τ_i are very close to the integral time-scales.

Fig. 8 presents values of τ_i^+ obtained in this way for $Pr = 0.1$, 0.3, 1, ∞. The values for $Pr = \infty$ are the time-scales calculated for fluid particles by Mito and Hanratty [17]. These results show a decrease in τ_i^+ with decreasing Pr. The τ_i^+ for $Pr = 1$ are seen to be very close to the values for $Pr = \infty$. Values of τ_i^+ obtained in this way for $Pr = 10$ are equal to the results for $Pr = \infty$.

Fig. 9 plots the ratio of τ_2 for a given Pr to the τ_2 obtained for $Pr = \infty$. These show that the assumption $\tau_2/\tau_{2,Pr=\infty}$ is constant over the whole channel cross-section would provide a good approximation for specifying τ_2^+ (x_2^+) for small Pr. The deviation of τ_i at very small x_2^+ is of no consequence because turbulence is having a negligible effect in this region. It is of interest to note that these results are similar to what has been found by Piller et al. [27] for turbulent diffusivities. Table 1 gives values of the ratio of the average turbulent diffusivities, α_t, over the whole cross-section of the channel,

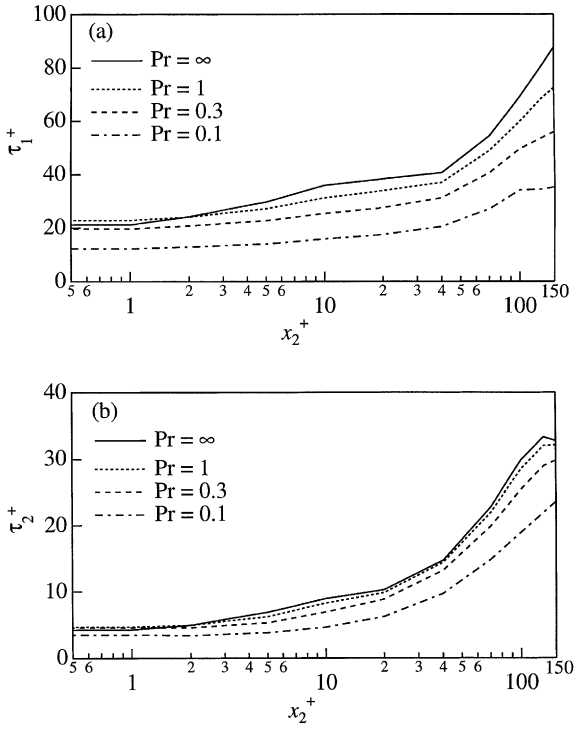

Fig. 8. Plots of Lagrangian time-scales: (a) τ_1^+ and (b) τ_2^+.

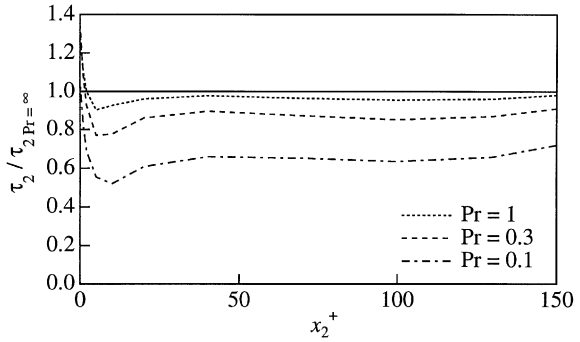

Fig. 9. Plots of ratios of Lagrangian time-scales to the values for fluid particles.

Table 1
Ratio of turbulent diffusivities to the value for $Pr = 1$ [27] and ratio of Lagrangian time-scales in the wall-normal direction to the value for $Pr = 1$

Pe_τ	Re_τ	$\alpha_t/\alpha_{t,Pr=1}$	$\tau_2/\tau_{2,Pr=1}$
15	150	0.67	0.68
15	300	0.66	–
45	150	0.84	0.90
150	150	1	1

except for the conductive sublayer. These are presented as the ratio of α_t for a given $Pr < 1$ to the α_t obtained for $Pr = 1$. The Peclet number, Pe_τ, is the product of Re_τ and Pr. Values of the spatial average of the ratio of τ_2^+ obtained from data in Fig. 8 outside the conductive sublayer are also given in Table 1. Of particular interest is recognition that $\tau_2/\tau_{2,Pr=1}$ is very close to the ratio, $\alpha_t/\alpha_{t,Pr=1}$.

6.2. Use of the Langevin equation to predict dispersions from an instantaneous point source

The modified Langevin equation was used to calculate dispersion from instantaneous point sources located at $x_2^+ = 0$, 1, 2, 5, 10, 20, 40, 70, 100, 130, 150. Good agreement was obtained between wall-normal concentration profiles determined in the experiments done with a DNS. This is illustrated in Figs. 3 and 5 for sources located at $x_2^+ = 40$ and at the wall. Good agreement with the DNS experiments was also obtained for streamwise dispersions for all cases except those for which the source was located at the wall and at $x_2^+ = 1$. This is illustrated in Fig. 4 for the case in which the instantaneous source was located at $x_2^+ = 40$. Fig. 7 compares streamwise dispersions from wall sources. This shows significant differences between the DNS and the calcu-

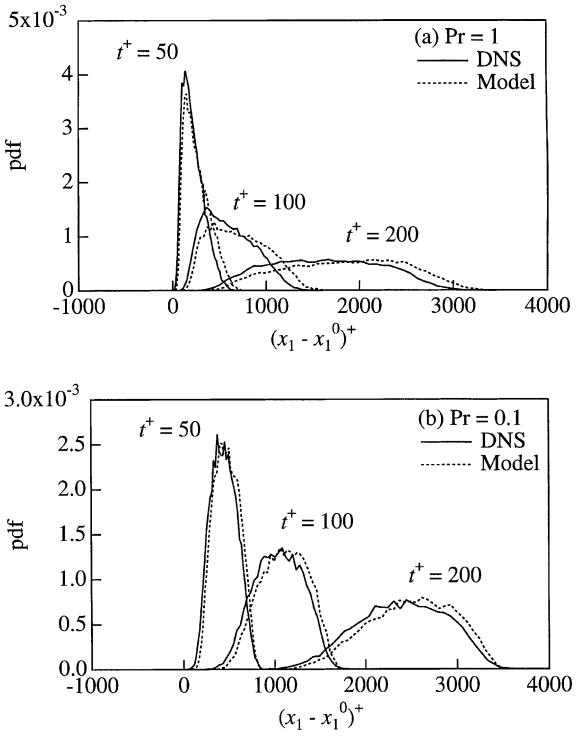

Fig. 10. Streamwise dispersion of wall sources for (a) $Pr = 1$ and (b) $Pr = 0.1$. Influence of streamwise velocity fluctuation was ignored.

lations at small times. However, good agreement is obtained at large times ($t^+ \geqslant 200$).

Dispersion in the streamwise direction occurs mainly because lateral mixing causes the thermal markers to see different mean velocities (Taylor diffusion). However, turbulent velocity fluctuations in the streamwise direction also play an important role. The poor agreement between the model and the DNS experiments seen in Fig. 7 could indicate that the model is overpredicting the contribution of streamwise velocity fluctuations close to the wall. This interpretation was investigated by neglecting the contribution of streamwise fluctuations. Thus dispersion in the streamwise direction is due only to Taylor diffusion and to molecular diffusion. The results of calculations carried out in this way are presented for a wall source in Fig. 10. The agreement with experiments done in a DNS is much better than shown in Fig. 7, at small times. The agreement at large times could be improved if the influence of turbulent velocity fluctuations in the streamwise direction were considered.

6.3. Fully developed temperature profiles

Values of temperature T^+ calculated as resulting from contributions of instantaneous hot sources between $t_1^+ = 0$ and $t_1^+ = t^+$ were calculated with (13), (15) and the probability distribution functions in Fig. 5. Fig. 11 compares $T^+(x_2^+, t^+)$ obtained by using the Langevin model and experimental results obtained in the DNS to represent P^+. Both solutions give $dT^+/dx_2^+ = -Pr$ at $x_2^+ \to 0$. Thus larger temperature gradients and larger temperatures are calculated at the wall for $Pr = 1$ than for $Pr = 0.1$. The temperature gradient at the other wall, $x_2^+ = 300$, is zero because a no flux condition was maintained there. The agreement between calculations made with the Langevin equation and results from the DNS experiment is good, but not perfect. The small differences could reflect limitations in the model or could suggest that Lagrangian time-scales, τ_2, should have been slightly modified.

Fig. 12 shows calculations for $t^+ = 2750$ for the case in which one wall is heated and the other is cooled. The Lagrangian representation considers the bottom wall ($x_2^+ = 0$) to consist of a series of sources and the top wall as a series of sinks. The temperature profile is the sum of these two contributions. The curves in Fig. 11 would represent the heat sources. A modification which substitutes $-T^+$ for T^+ and $(300 - x_2^+)$ for x_2^+ represents the cold sources. Fig. 12 presents the stationary state that is reached at large t^+. The agreement between calculations in which the Langevin equation and experiments in a

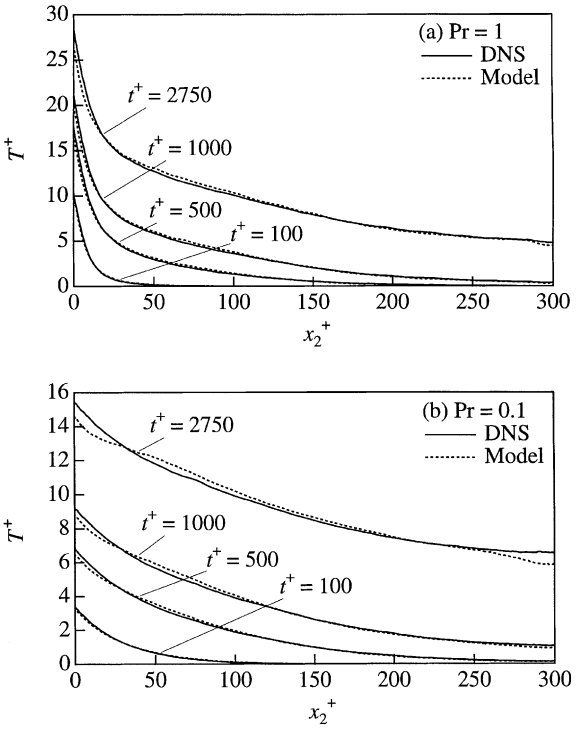

Fig. 11. Temperature profiles for the boundary condition of a constant heat flux for (a) $Pr = 1$ and (b) $Pr = 0.1$.

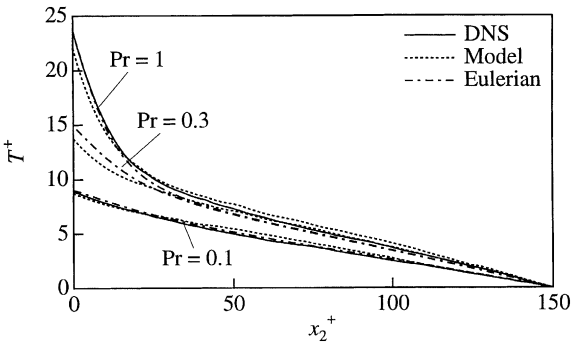

Fig. 12. Fully developed mean temperature profiles.

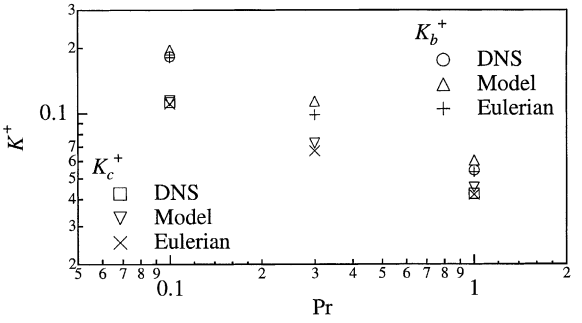

Fig. 13. Dimensionless heat transfer coefficients, where K_b and K_c indicate the use of temperature driving forces defined with the bulk temperature and the centerline temperature.

DNS are used to represent probability distribution functions is again good, but not perfect.

Dimensionless heat transfer coefficients, K_b^+ and K_c^+, are plotted in Fig. 13. The symbols $\times$ and $+$ represent DNS Eulerian calculations. The squares and circles represent Lagrangian calculation in which the probability density functions were obtained from DNS experiments and the triangles, calculations with the Langevin equation.

7. Concluding remarks

Mito and Hanratty [17] have shown that a modified form of the Langevin equation can be used to describe dispersion from a point source in a nonhomogeneous field. The system considered was turbulent flow in a channel. Information on the spatial variation of the Eulerian turbulence and on the spatial variation of a Lagrangian time-scale, τ_i, had to be specified. Correlations for τ_i were presented.

One possible use of this approach is the description of the temperature field generated by turbulent flow over a heated (or cooled) surface as resulting from an array of sources located on the wall. This is a more complicated problem than that considered by Mito and Hanratty [17] in that the results are more sensitive to the specification of the turbulence close to the wall and that molecular diffusion needs to be considered because this is the mechanism by which heat is transmitted from the wall to the fluid.

This paper shows how the work of Mito and Hanratty [17] can be extended to describe the behavior of a source on the wall. It shows for $Pe_\tau >$ ca 150 that τ_i for fluid particles can be used. For $Pe_\tau <$ ca 150 the τ_i will be lower than that for fluid particles. The fractional decrease can be considered to be roughly a constant and to be approximately equal to the decrease in the turbulent diffusivity.

Calculated wall-normal temperature profiles are in remarkably good agreement with experiments done in a DNS, considering that such a simple equation is used to represent a flow with so much complexity. The description of an instantaneous wall source can be used to describe a variety of problems with different configurations of the heat transfer surfaces. This is demonstrated in this paper for the fully developed temperature profile that can develop for turbulent flow through a channel with one heated and one cooled wall.

Acknowledgements

This work is supported by the DOE under grant DEF G02-86ER 13556 and by the NSF under grant NSF CTS-98-06265. Computer resources have been provided by the National Center for Supercomputer Applications (NCSA), Urbana.

References

[1] G.I. Taylor, Diffusion by continuous movements, Proc. London Math. Soc. 20 (1921) 196–211.
[2] P. Langevin, C.R. Acad. Sci. 146 (1982) 530.
[3] C.C. Lin, W.H. Reid, Turbulent flow, theoretical aspects, in: Encyclopedia of Physics 8/2, Springer-Verlag, Berlin, 1963, pp. 438–523.
[4] A.M. Obukhov, Description of turbulence in terms of Lagrangian variables, Adv. Geophys. 6 (1959) 113–116.
[5] P.A. Durbin, Stochastic differential equations and turbulent dispersion, NASA Ref. Publ. 1103 (1983).
[6] P.A. Durbin, Comment on papers by Wilson et al. (1981) and Legg and Raupach (1982), Bound. Lay. Meteorl. 29 (1984) 409–411.
[7] C.D. Hall, The simulation of particle motion in the atmosphere by a numerical random walk model, Q. J. R. Meteor. Soc. 101 (1975) 235–244.
[8] B.J. Legg, M.R. Raupach, Markov-chain simulation of particle dispersion in inhomogeneous flows: The mean drift velocity induced by a gradient in Eulerian velocity variance, Bound. Lay. Meteorl. 24 (1982) 3–13.
[9] J.D. Reid, Markov chain simulations of vertical dispersion in the neutral surface layer for surface and elevated releases, Bound. Lay. Meteorl. 16 (1979) 3–22.
[10] A.M. Reynolds, On the application of Thomson's random flight model to the prediction of particle dispersion within a ventilated airspace, J. Wind Eng. Ind. Aerod. 67–68 (1997) 627–638.
[11] D.J. Thomson, Random walk modelling of diffusion in inhomogeneous turbulence, Q. J. R. Meteor. Soc. 110 (1984) 1107–1120.
[12] D.J. Thomson, A random walk model of dispersion in turbulent flows and its application to dispersion in a valley, Q. J. R. Meteor. Soc. 112 (1986) 511–530.
[13] D.J. Thomson, Criteria for the selection of stochastic models of particle trajectories in turbulent flows, J. Fluid Mech. 180 (1987) 529–556.
[14] H. van Dop, F.T.M. Nieuwstadt, J.C.R. Hunt, Random walk models for particle displacements in inhomogeneous unsteady turbulent flows, Phys. Fluids 28 (1985) 1639–1653.
[15] J.D. Wilson, G.W. Thurtell, G.E. Kidd, Numerical simulation of particle trajectories in inhomogeneous turbulence, II: systems with variable turbulent velocity scale, Bound. Lay. Meteorl. 21 (1981) 423–441.
[16] I. Iliopoulos, T.J. Hanratty, Turbulent dispersion in a nonhomogeneous field, J. Fluid Mech. 392 (1999) 45–71.
[17] Y. Mito, T.J. Hanratty, Use of a modified Langevin equation to describe turbulent dispersion of fluid particles in a channel flow, Flow Turbul. Combust. 68 (2002) 1–26.
[18] S. Chandrasekhar, Stochastic problems in physics and astronomy, Rev. Modern Phys. 15 (1) (1943).
[19] K. Kontomaris, T.J. Hanratty, Effect of molecular diffusivity on point source diffusion in the center of a numer-

ically simulated turbulent channel flow, Int. J. Heat Mass Tran. 37 (13) (1994) 1817–1828.
[20] T.J. Hanratty, Heat transfer through a homogeneous isotropic turbulent field, A.I.Ch.E. J. 2 (1956) 42–45.
[21] D.V. Papavassiliou, T.J. Hanratty, Transport of a passive scalar in a turbulent channel flow, Int.J. Heat Mass Tran. 40 (6) (1997) 1303–1311.
[22] D.V. Papavassiliou, T.J. Hanratty, The use of Lagrangian methods to describe turbulent transport of heat from a wall, Ind. Eng. Chem. Res. 34 (1995) 3359–3367.
[23] S.L. Lyons, T.J. Hanratty, J.B. McLaughlin, Large-scale computer simulation of fully developed turbulent channel flow with heat transfer, Int. J. Numer. Methods Fluids 13 (1991) 999–1026.
[24] K. Kontomaris, T.J. Hanratty, J.B. McLaughlin, An algorithm for tracking fluid particles in a spectral simulation of turbulent channel flow, J. Comput. Phys. 103 (1992) 231–242.
[25] H.S. Carslaw, J.C. Jaeger, Conduction of Heat in Solids, second ed., Oxford, New York, 1959.
[26] A.S. Monin, A.M. Yaglom, in: Statistical Fluid Mechanics, vol.1, MIT Press, Cambridge, 1975.
[27] M. Piller, E. Nobile, T.J. Hanratty, DNS study of turbulent transport at low Prandtl numbers in a channel flow, J. Fluid Mech. 458 (2002) 419–441.